# ANCA: A Family of Fluorescent Probes that Bind and Stain Amyloid Plaques in Human Tissue

Willy M. Chang,[†] Marianna Dakanali,[†] Christina C. Capule,[†] Christina J. Sigurdson,[‡] Jerry Yang,*,[†] and Emmanuel A. Theodorakis*,[†]

[†]Department of Chemistry & Biochemistry, University of California, San Diego, 9500 Gilman Drive MC: 0358, La Jolla, California 92093-0358, United States

[‡]Department of Pathology, University of California, San Diego, 9500 Gilman Drive MC: 0612, La Jolla, 92093-0612, United States

Ⓢ *Supporting Information*

ABSTRACT: A new family of fluorescent markers containing an amino naphthalenyl-2-cyano-acrylate (ANCA) motif has been synthesized and evaluated for its capability to associate with aggregated β-amyloid (Aβ) peptides. These fluorescent probes contain a nitrogen donor group that is connected via a naphthalene unit to an electron acceptor motif containing water solubilizing groups (WSGs). Chemical modifications were introduced to explore their effect on the capability of the ANCA-based probes to fluorescently label aggregated Aβ peptides. All synthesized probes bind to aggregated Aβ fibrils with low micromolar affinity and fluorescently stain

amyloid deposits in human brain tissue from patients with Alzheimer's disease. We found that structural modifications of the WSG site do not affect considerably the binding affinity. However, changes of the nitrogen donor group alter significantly the binding affinity of these probes. Also, increasing the hydrophilicity of the donor group leads to improved contrast between the Aβ deposits and the surrounding tissue in histological staining experiments.
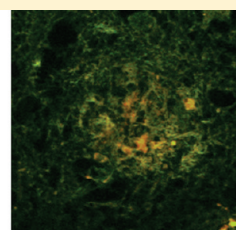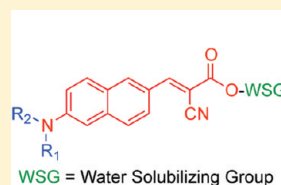
KEYWORDS: Molecular rotor, fluorescence, imaging agents, amyloid peptide, Alzheimer's disease

Alzheimer's disease (AD) is a neurodegenerative disorder characterized by a progressive impairment of episodic memory and language deficits.[1] Pathologically, AD is characterized by accumulation of amyloid-β (Aβ) deposits in the brain. The major component of these deposits are Aβ40 and Aβ42 peptides that are derived from amyloid precursor protein after cleavage by β- and γ-secretases.[2] To date, the late-stage diagnosis of AD is achieved using functional memory and behavioral tests;[3] early stage asymptomatic diagnosis, however, remains a challenge. Along these lines, recent efforts have targeted the visualization of amyloid deposits in vivo. Moreover, the structure of a model amyloidogenic peptide that sustains the property of aggregation has been proposed.[4,5] In turn, this paves the way for a rational design of amyloid-binding molecules that can potentially be used for in vivo and ex vivo imaging. Such molecules not only can help evaluate the time course and evolution of the disease, but also can allow for the timely monitoring of therapeutic treatment.[6−8]

Over the past few years a number of probes have been developed for the specific labeling and imaging of the Aβ plaques. These probes rely on techniques such as magnetic resonance imaging (MRI),[9,10] positron emission tomography (PET),[11−14] and single photon emission computed tomography (SPECT).[15,16] In addition, fluorescent probes that can stain Aβ deposits have gained increasing interest as potential tools for monitoring the progression of AD in vitro and in vivo. In principle, such fluorescent probes are advantageous over PET/SPECT methods, since they provide real-time, nonradioactive, and high-resolution

imaging both in vivo and ex vivo. Figure 1 illustrates representative structures of such probes that, to-date, have found limited use as fluorescent labeling agents of Aβ deposits in small animal studies.[17−22] Reliable methods to fine-tune the optical and biocompatible properties of these amyloid-targeting agents and to improve their selectivity and affinity to amyloid deposits in tissue could further advance this optical strategy for AD monitoring and diagnosis. In general, an appropriate fluorescent probe for amyloids should have the following properties:[11,18,21] (a) molecular mass less than 600 Da, (b) emission wavelength above 450 nm to minimize background fluorescence from brain tissue[23] (c) high quantum yield, (d) appropriate lipophilicity (log P value between 1 and 3), (e) specificity to Aβ plaques, (f) sufficient binding affinity to aggregated amyloid peptides, (g) straightforward synthesis, and (h) upon binding to Aβ deposits, a significant change in fluorescent properties should be observed.

Recently, we reported the rational design of a new class of amyloid-binding agents based on the molecular rotor motif.[24,25] This motif contains an electron-donor unit in conjugation with an electron acceptor and produces a fluorescence quantum yield that is dependent on the surrounding environment. Hindrance of the internal molecular rotation of the probe, by increasing the
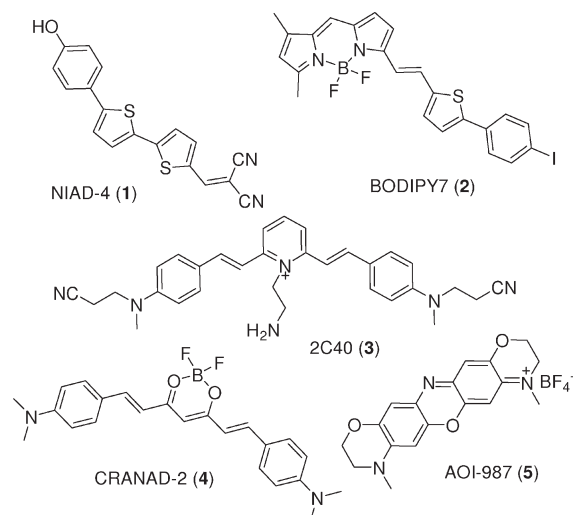
Figure 1. Examples of fluorescent probes that stain Aβ deposits in tissue.
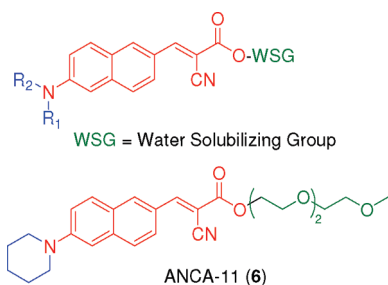

Figure 2. General motif of the ANCA probes. The ANCA scaffold is shown in red. Substitutions at the nitrogen and the WSG sites are shown in blue and green, respectively.

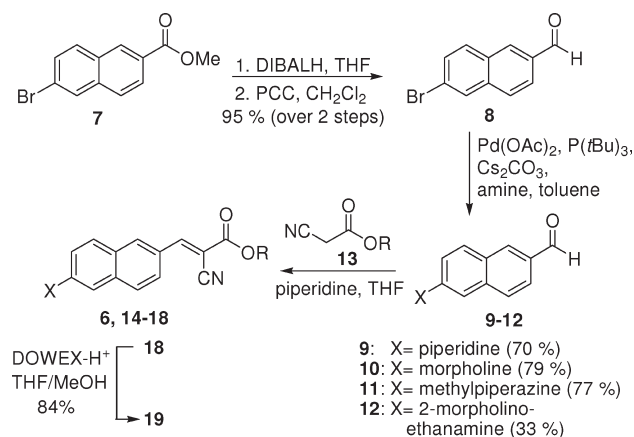**Scheme 1. General Strategy for the Synthesis of Probes 6 and 14–19**

Table 1. Structures of ANCA-Based Aβ-Binding Probes and Their Isolated Yields after Reaction of 9–12 with 13

Compound	X	R	Yield (%)
6			90
14			85
15			83
16			87
17			89
18			83
19			84[a]

[a] Yield refers to conversion of compound 18 to 19.

surrounding media rigidity or by reducing the available free volume needed for relaxation, leads to a decrease in the non-radiative decay rate and consequently an increase of fluorescent emission. Closer evaluation of the data led to the identification of 6-aminonapthalenyl-2-cyano-acrylate (ANCA) as a motif with potentially useful spectroscopic properties for fluorescent labeling of aggregated amyloids peptides (Figure 2). Specifically, compound 6, referred to as ANCA-11, possesses a long emission wavelength and large increase in fluorescence intensity upon binding to Aβ fibrils.[24] In order to validate the ANCA scaffold as a general motif that can bind to aggregated Aβ peptides, we sought to examine whether structural changes at its periphery, including alterations at the water solubilizing groups or at the nitrogen substitution, can affect the binding and fluorescent properties of the probe. Herein, we present the synthesis and the optical properties of a small family of compounds based on the ANCA motif. The ex vivo staining of amyloid plaques in human tissue by these novel fluorescent probes is also presented.

A general strategy for the synthesis of all ANCA-based probes is depicted in Scheme 1. Commercially available methyl 6-bromo-naphthalene-2-carboxylate (7) was converted to the corresponding naphthaldehyde 8 by reduction of the ester to the primary alcohol using DIBALH and oxidation of the resulting alcohol to the desired aldehyde upon treatment with PCC.[26] The transformation of the bromide to the appropriate amine demanded the use of novel

chemistry to improve the yield and apply the method in bigger scale. To this end, treatment of bromide 8 in the presence of palladium using Buchwald and Hartwig conditions produced aldehydes 9–12 in excellent yield for most cases.[27–29] Knövenagel condensation of aldehydes 9–12 with the appropriate cyanoester 13 concluded the synthesis of the final probes 6 and 14–18, as a single stereoisomer (E isomer).[30] Deprotection of the acetal group of 18 using acidic resin yielded the final dye 19.

Table 1 summarizes the R and X combinations of the final products and the condensation yields. Based on their chemical structures, the synthesized probes can be separated in two subgroups: compounds 6, 17, and 19 (group A) that contain an identical piperidine donor group and differ only in the water solubilizing group (WSG) area (triethylene glycol monomethyl ether, tetraethylene glycol monomethyl ether, and propane 1,2-diol motif, respectively), and compounds 6, 14, 15, and 16 (group B) that contain an identical WSG motif (triethylene glycol monomethyl ether) but differ in the nitrogen substitution.

To be useful, a fluorescent amyloid-binding probe should display a significant increase in fluorescence emission upon binding with the aggregates as compared to the emission of the free probe in solution.[31] To test whether the ANCA family of probes possessed these desirable fluorescence properties, we compared the fluorescent properties of all free probes in aqueous solution to their fluorescence properties in the presence of aggregated Aβ42 peptides. We chose to evaluate the binding of probes to Aβ42 instead of Aβ40, since Aβ42 is the major amyloid species found in AD plaques.[2,32−34] Specifically, we evaluated the fluorescent properties of each probe at a final concentration of 4 μM in nanopure water, before and after mixing with aggregated Aβ42 peptide (final concentration peptide = 5 μM). As shown in Table 2, in all cases, we observed a significant increase (2.9−8.4-fold) in the intensity of the emission spectra of the probes upon association with the aggregated amyloid peptides.[35] This intensity increase was also accompanied by a blue shift in the emission spectra of around 5−50 nm. After binding, all compounds had excitation maxima between 380 and 430 nm and their emission maxima were between 525 and 550 nm, suggesting that small changes in the donor or acceptor part of the molecule do not alter significantly their fluorescent maxima. However, compounds **6**, **17**, and **19** (group A), that possess piperidine as the electron donor, showed higher increase in fluorescence intensity after binding (7.7-, 8.4-, and 6.6-fold, respectively) as compared to

probes containing piperazine (**14**), morpholine (**15**), or morpholino-ethanamine (**16**) groups as electron donors (group B). Figure 3 provides a representative example of the fluorescent properties of compound **14**.

We also measured the apparent binding constants (K_d) of the probes to aggregated Aβ42 peptides. The fluorescent intensity of each probe was measured at concentrations of 1.25, 2.5, 5.0, and 10 μM in nanopure water, mixed with preaggregated Aβ42 peptides (final concentration of peptide = 5 μM).[36] In all cases, the K_d values were between 1.4 and 13.8 μM. Interestingly, group A exhibited the highest affinity to aggregated Aβ peptides. The nearly identical K_d values obtained for these dyes (1.4−1.6 μM) indicate that small chemical modifications within the water-solubilizing region of the ANCA motif do not affect significantly the binding of the probes to Aβ aggregates. On the other hand, a measurable change of the K_d value was observed upon chemically altering the electron donor moiety of the ANCA motif. As shown in Table 2, compounds having piperidine as the electron donor were found to have lower K_d values (1.4−1.6 μM) compared to those possessing piperazine, morpholine, or morpholino-ethanamine as electron donor (compounds **14**, **15**, and **16** respectively).

Finally, the lipophilicity (log P) of the synthesized probes was calculated.[37] All compounds were found to have log P values between 2.5 and 3.8, suggesting that most of them possess the desirable properties for biocompatibility and can potentially cross the blood brain barrier.[38]

In order to assess whether this family of ANCA-based fluorescent probes could stain amyloid deposits in brain tissue, we exposed sections of frozen human brain tissue (derived from the cerebral cortex of AD cases) to solutions containing the fluorescent probes. Figure 4 shows representative examples of fluorescence micrographs of these tissue samples incubated with each probe. As can be seen in Figure 4, all tissue samples exposed to the ANCA probes contained small regions within the tissue that exhibited a significant concentration of fluorescence. As a negative control, we exposed frozen tissue sections to control vehicle (DMSO/PBS buffer) and did not observe such concentrated areas of fluorescence (data not shown).
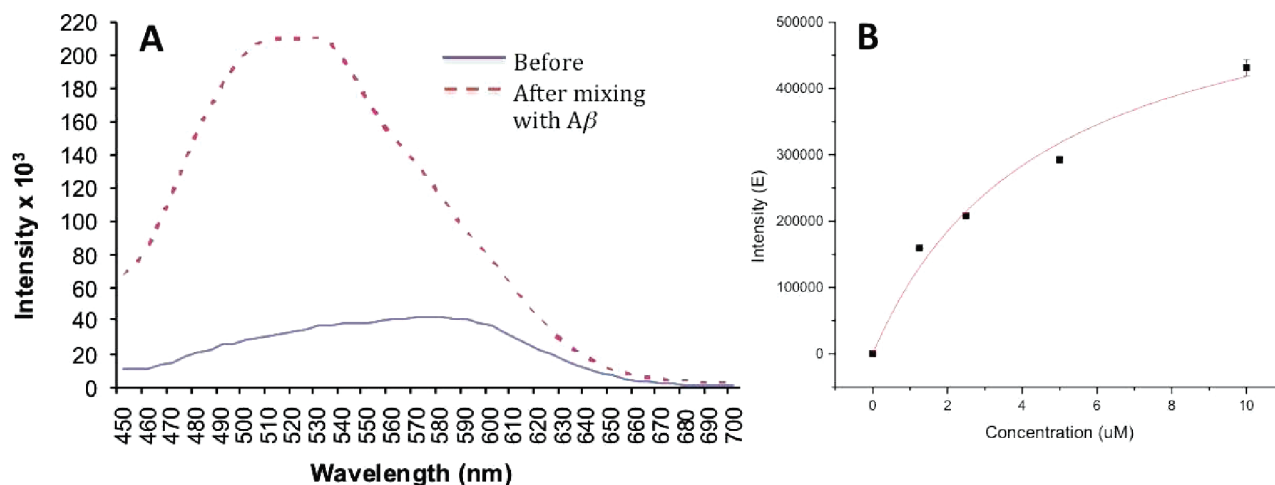
Table 2. Fluorescence Profile, K_d and log P Values of the Synthesized Probes with Aggregated Aβ(1-42) peptides

cmpd no.	exc. max (nm)		em. max (nm)		fold increase	K_d (μM)	log P^a
	before	after	before	after			
6	415	410	590	545	7.7	1.4 ± 0.2	3.81
14	400	385	570	530	5.0	4.6 ± 1.3	2.79
15	400	380	530	525	5.1	13.8 ± 3.1	2.74
16	430	430	570	540	2.9	6.7 ± 2.1	2.53
17	420	410	590	550	8.4	1.6 ± 0.9	3.60
19	410	410	545	535	6.6	1.6 ± 0.2	3.14

^{a} Log P values were calculated with Molinspiration Cheminformatics Software.

Figure 3. (A) Fluorescent emission of compound **14** before (blue solid line) and after (red dotted line) mixing with Aβ aggregates. (B) Plot of the fluorescence intensity (at λ = 530 nm) as a function of the concentration of compound **14** in the presence of aggregated Aβ42 peptides (5 μM) in solution. Fitting this data to the equation: $y = Bx/(K_d + x)$ revealed a K_d of 4.6 ± 1.3 μM for association of compound **14** to aggregated Aβ42 peptides.
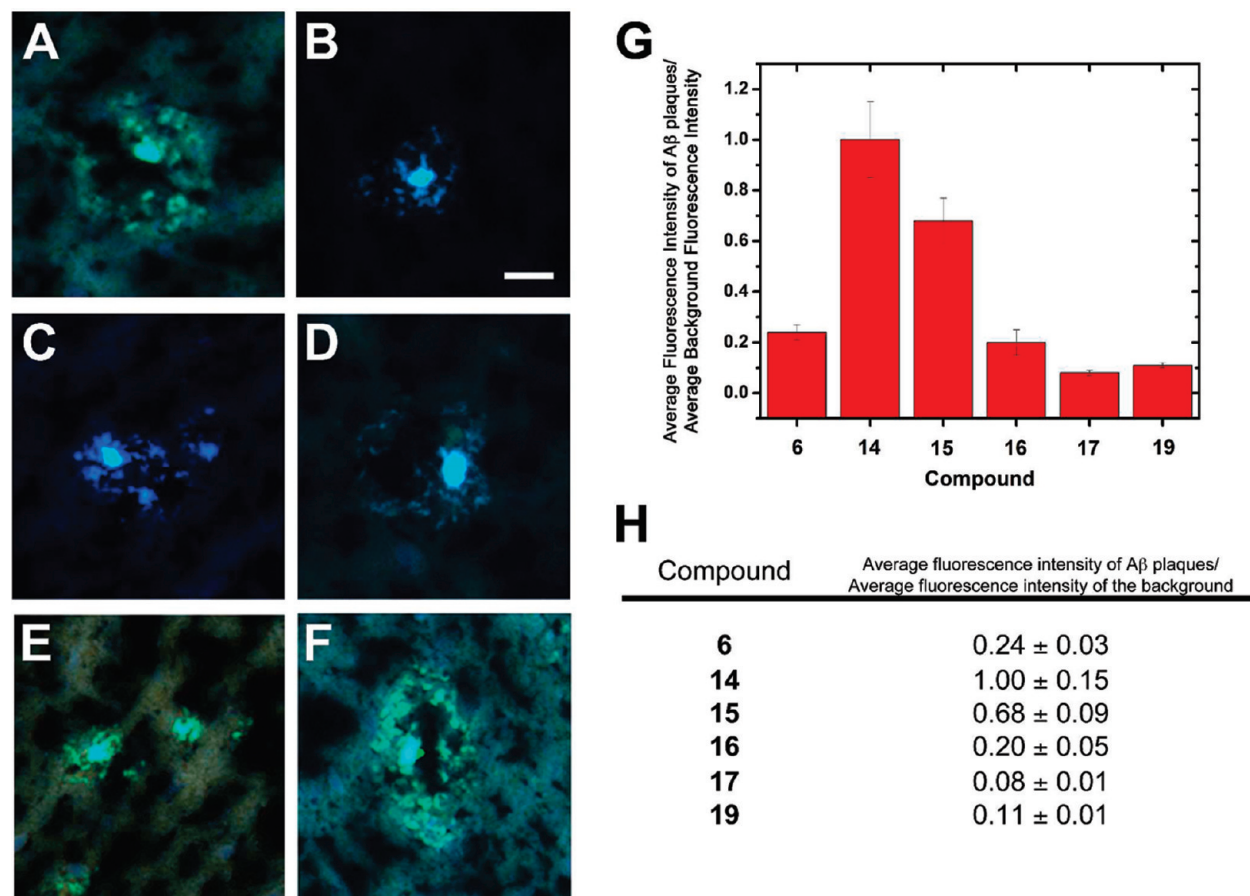
Figure 4. Staining of Aβ plaques in brain sections from an AD patient. Frozen brain sections mounted on glass slides were dried and briefly fixed in ethanol, immersed in PBS, exposed to a 60 μM solution of fluorescent probe in PBS for 30 min, washed with PBS, and covered with a glass coverslip. Plaques from brain sections were stained with (A) compound 6, (B) compound 14, (C) compound 15, (D) compound 16, (E) compound 17, or (F) compound 19. Stained Aβ plaques were imaged using a Leica DM IRE2 inverted epifluorescence microscope equipped with a Hamamatsu camera. Images from the blue, red, and green filters were overlaid. (G) Graphical representation of the average fluorescence intensity of the probes bound to amyloid plaques relative to the fluorescence intensity of the background. All data is presented relative to the fluorescence contrast for staining plaques with compound 14. The data represents the mean relative fluorescence intensity ± SD ($n = 10$ measurements for each compound). (H) Table of the average fluorescence intensity of the plaques in (A−F) relative background. All data was normalized to the average fluorescence intensity of plaques stained with compound 14 relative to background. Scale bar = 20 μm.

More interestingly, inspection of the images from these staining experiments (Figure 4) reveals a trend of increased fluorescent labeling of amyloid plaques using probes 14 and 15 compared to all other probes (Figure 4G). This trend can be seen by increased fluorescence contrast between the plaques and surrounding tissue in Figure 4B, C (corresponding to tissue samples stained with compounds 14 and 15) compared to the weaker observed contrast between the plaques and the surrounding tissue shown in Figure 4A, D−F (corresponding to tissue samples stained with compounds 6, 16, 17, and 19). We hypothesize that the improved contrast of amyloid deposits stained with probes 14 and 15 may be attributed to their increased hydrophilicity compared to 6, 16, 17, and 19. The increased hydrophilic properties of 14 and 15 could reduce the amount of nonspecific staining by these probes to the brain tissue. This effect would result in the observed trend for increased fluorescence contrast between the plaques and surrounding tissue when using the more hydrophilic fluorescent probes.

In addition, Figure 5A−C shows representative fluorescence micrographs of a single formalin-fixed tissue sample from a human AD patient that was treated sequentially with a mouse monoclonal anti-human Aβ IgG (clone 82E1), a fluorescently labeled polyclonal anti-mouse IgG, and a solution containing probe 15. The bright green areas in Figure 5A indicate the regions of tissue that are labeled by compound 15, the bright red areas in Figure 5B indicate the regions of the tissue that are labeled by the anti-Aβ IgGs, and the bright yellow areas in Figure 5C represent the regions where probe 15 and the anti-Aβ IgGs overlap in the tissue. The images in Figure 5A−C reveal that the fluorescent ANCA probes label the amyloid deposits with good specificity in these human tissue sections. These staining experiments strongly support the notion that the ANCA-based probes are capable of marking the location of amyloid deposits within human brain tissue.

In conclusion, we show that the amino naphthalenyl-2-cyanoacrylate (ANCA) motif has appropriate fluorescence characteristics for the targeting and staining of Aβ deposits in tissue. Functionalization of this motif with water solubilizing groups does not affect the binding to Aβ but can help with the biocompatibility and water-solublizing properties of the compounds.[37,39] On

252

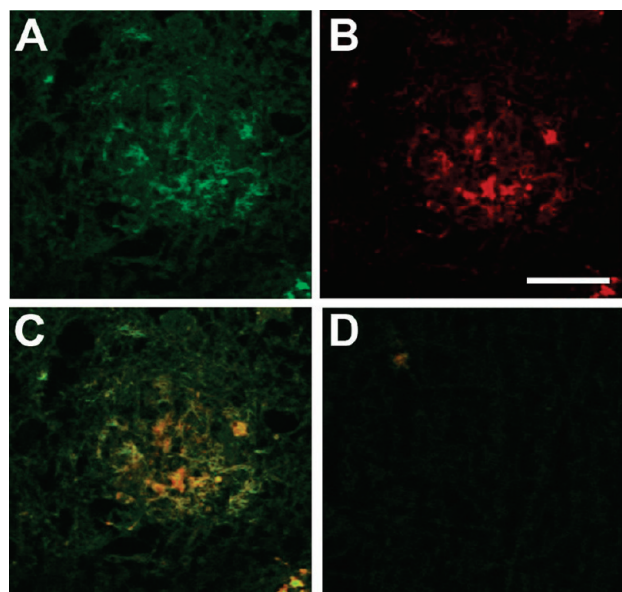dx.doi.org/10.1021/cn200018v |ACS Chem. Neurosci. 2011, 2, 249–255

Figure 5. Fluorescence micrographs of formalin-fixed brain sections from an AD patient revealing amyloid plaques that are labeled with (A) probe **15** or (B) a monoclonal anti-Aβ IgG (clone 82E1). (C) A fluorescence micrograph representing regions of overlap (yellow) for the fluorescence labeling of tissue by probe **15** and the anti-Aβ IgG. No labeling was observed in the IgG isotype/DMSO stained isotype control section (D). Scale bar = 20 μm.

the other hand, changes in the nitrogen motif can significantly affect the binding affinity and specificity of the probes to Aβ deposits in tissue. Based on the above results, we can propose that the donor part of the molecule is most likely located within the binding pocket of the aggregated protein. Thus, any changes in that domain can affect the interactions between the small molecule and protein. Ongoing efforts in our lab are aiming to further support this hypothesis.

METHODS

Synthesis and Spectroscopic Characterization of New Compounds. Synthetic procedures and spectroscopic data for all compounds are included in the Supporting Information.

Fluorescence Studies with Aggregated Aβ Peptides. Aggregated Aβ peptide was prepared as described previously.[24] Briefly, we dissolved Aβ42 in PBS pH 7.4 to a final concentration of 100 μM. This solution was magnetically stirred at 1200 rpm for 3 days at room temperature. Aliquots of 15 μL of the preaggregated Aβ42 solution were added to 285 μL of the probe (5% DMSO in nanopure water) to attain a final concentration of 5 μM A$\beta(1-42)$ and 4 μM of the probe. The solution was transferred to a 300 μL cuvette, and the fluorescence was measured.

Determination of Binding Constant. Preaggregated Aβ42 (5 μM final concentration) was mixed with various concentrations of probes (10, 5, 2.5, 1.25 μM) in 5% DMSO in nanopure water, and their K_d's were determined as described previously.[24]

Patient Samples. AD cases were from the Alzheimer Disease Research Center (ADRC) at the University of California, San Diego (UCSD). Subjects came to autopsy between 1985 and 2006 and postmortem interval for the cases was under 12 h. Institutional board review was obtained from the UCSD Human Research Protections Program, in accordance with the Health Insurance Portability and Accountability

Act. Written informed consent was obtained from all patients or their guardians.

Staining of Human Tissue Sections. Frozen brain sections from patients diagnosed with AD were dried for 1 h, treated with 100%, 95%, and 70% ethanol for 5 min each, and then rinsed in deionized water. The sections were equilibrated in phosphate-buffered saline (PBS) for 15 min. Fluorescent molecules were diluted in PBS (1:50, from stock solutions of 3 mM in PBS to give a final concentration of 60 μM), added to the brain sections, incubated for 30 min at room temperature, washed with PBS, and coverslipped.

Costaining with the Aβ Antibody 82E1 and Compound 15. Aβ and compound **15** costaining was performed on a formalin-fixed brain section from an AD case. Slides were deparaffinized, incubated for 5 min in 98% formic acid, and then washed in distilled water for 5 min. Sections were blocked with 10% goat serum and incubated with anti-Aβ antibody 82E1 (Immunobiological Laboratories) for 30 min. The slides were washed with PBS containing 0.2% tween and stained with antibody anti-mouse HRP (Jackson Immunolabs), washed in PBS-tween, and tyramide-Alexa Fluor 594 (Invitrogen) for 30 min. After washing with PBS-tween, the slides were stained with 60 μM solutions of compound **15** for 30 min. Control sections were costained with the mouse isotype control antibody as the primary antibody, and the PBS control buffer that was used to generate stock solutions of compound **15**. Adjacent sections were singly stained with Aβ antibody 82E1 or compound **15**.

Fluorescence Microscopy. The sample was excited using an argon 488 nm laser on an Olympus FluoView FV1000 confocal microscope. The emission spectra of the probes bound to Aβ or background were collected in 5 nm increments from 450−645 nm. A minimum of 10 measurements were collected for probe bound to Aβ and for background. The peak intensity for the Aβ-bound probe was divided by an average of the background measurements to calculate the ratio of probe to background signal.

ASSOCIATED CONTENT

ⓢ Supporting Information. Synthetic procedures, spectroscopic and analytical characterization, including copies of ^{1}H NMR and ^{13}C NMR spectra, of compounds **8−19**. Fluorescent spectra of compounds **6**, **14−17**, and **19** with aggregated Aβ peptide. Raw data from fluorescence experiments used to estimate the K_d's of **6**, **14−17**, and **19** for binding to aggregated Aβ peptides. This material is available free of charge via the Internet at http://pubs.acs.org.

AUTHOR INFORMATION

Corresponding Author
*(J.Y.) E-mail: jerryyang@ucsd.edu. Telephone: 858-534-6006. Fax: 858-534-4554. (E.A.T.) E-mail: etheodor@ucsd.edu. Telephone: 858-822-0456. Fax: 858-822-0386.

Author Contributions
E.A.T., J.Y., and C.J.S. conceived the overall project. M.D. and E. A.T. designed the small molecule synthesis. W.M.C. performed the synthesis experiments. C.C.C. and W.M.C. performed the fluorescence binding studies. C.J.S. designed and performed the ex vivo fluorescence imaging studies.

■ ACKNOWLEDGMENT

■ REFERENCES

(1) Minati, L., Edginton, T., Bruzzone, M. G., and Giaccone, G. (2009) Current concepts in Alzheimer's Disease: A multidisciplinary review. Am. J. Alzheimers Dis. 24, 95–121.

(2) Selkoe, D. J. (1999) Translating cell biology into therapeutic advances in Alzheimer's disease. Nature 399, A23–31.

(3) Dubois, B., Feldman, H. H., Jacova, C., DeKosky, S. T., Barberger-Gateau, P., Cummings, J., Delacourte, A., Galasko, D., Gauthier, S., Jicha, G., Meguro, K., O'Brien, J., Pasquier, F., Robert, P., Rossor, M., Salloway, S., Stern, Y., Visser, P. J., and Scheltens, P. (2007) Research criteria for the diagnosis of Alzheimer's disease: revising the NINCDS—ADRDA criteria. Lancet Neurol. 6, 734–746.

(4) Mathis, C. A., Wang, Y., and Klunk, W. E. (2004) Imaging β-amyloid plaques and neurofibrillary tangles in the aging human brain. Curr. Pharm. Des. 10, 1469–1492.

(5) Kim, Y. S., Lee, J. H., Ryu, J., and Kim, D. J. (2009) Multivalent & multifunctional ligands to β-amyloid. Curr. Pharm. Des. 15, 637–658.

(6) Nichols, L., Pike, V. W., Cai, L., and Innis, R. B. (2006) Imaging and in vivo quantitation of β-amyloid: An exemplary biomarker for Alzheimer's disease?. Biol. Psychiatry 59, 940–947.

(7) Matthews, B., Siemers, E. R., and Mozley, P. D. (2003) Imaging-based measures of disease progression in clinical trials of disease-modifying drugs for Alzheimer disease. Am. J. Geriatr. Psychiatry 11, 146–159.

(8) Golde, T. E., and Bacskai, B. J. (2005) Bringing amyloid into focus. Nat. Biotechnol. 23, 552–554.

(9) Higuchi, M., Iwata, N., Matsuba, Y., Sato, K., Sasamoto, K., and Saido, T. C. (2005) ^{19}F and ^{1}H MRI detection of amyloid β plaques in vivo. Nat. Neurosci. 8, 527–533.

(10) Poduslo, J. F., Curran, G. L., Peterson, J. A., McCormick, D. J., Fauq, A. H., Khan, M. A., and Wengenack, T. M. (2004) Design and chemical synthesis of a magnetic resonance contrast agent with enhanced in vitro binding, high blood-brain barrier permeability, and in vivo targeting to Alzheimer's disease amyloid plaques. Biochemistry 43, 6064–6075.

(11) Klunk, W. E., Engler, H., Nordberg, A., Wang, Y., Blomqvist, G., Holt, D. P., Bergström, M., Savitcheva, I., Huang, G.-F., Estrada, S., Ausén, B., Debnath, M. L., Barletta, J., Price, J. C., Sandell, J., Lopresti, B. J., Wall, A., Koivisto, P., Antoni, G., Mathis, C. A., and Långström, B. (2004) Imaging brain amyloid in Alzheimer's disease with Pittsburgh Compound-B. Ann. Neurol. 55, 306–319.

(12) Stephenson, K. A., Chandra, R., Zhuang, Z. P., Hou, C., Oya, S., Kung, M. P., and Kung, H. F. (2007) Fluoro-pegylated (FPEG) imaging agents targeting Aβ aggregates. Bioconjugate Chem. 18, 238–246.

(13) Nordberg, A. (2007) Amyloid imaging in Alzheimer's disease. Curr. Opin. Neurol. 20, 398–402.

(14) Johnson, A. E., Jeppsson, F., Sandell, J., Wensbo, D., Neelissen, J. A. M., Juréus, A., Ström, P., Norman, H., Farde, L., and Svensson, S. P. S. (2009) AZD2184: a radioligand for sensitive detection of β-amyloid deposits. J. Neurochem. 108, 1177–1186.

(15) Newberg, A. B., Wintering, N. A., Plossl, K., Hochold, J., Stabin, M. G., Watson, M., Skovronsky, D., Clark, C. M., Kung, M.-P., and Kung, H. F. (2006) Safety, biodistribution, and dosimetry of 123I-IMPY: A novel amyloid plaque-imaging agent for the diagnosis of Alzheimer's disease. J. Nucl. Med. 47, 748–754.

(16) Kung, M.-P., Hou, C., Zhuang, Z.-P., Zhang, B., Skovronsky, D., Trojanowski, J. Q., Lee, V. M. Y., and Kung, H. F. (2002) IMPY: an improved thioflavin-T derivative for in vivo labelling of β-amyloid plaques. Brain Res. 956, 202–210.

(17) Hintersteiner, M., Enz, A., Frey, P., Jaton, A.-L., Kinzy, W., Kneuer, R., Neumann, U., Rudin, M., Staufenbiel, M., Stoeckli, M., Wiederhold, K.-H., and Gremlich, H.-U. (2005) In vivo detection of amyloid-β deposits by near-infrared imaging using an oxazine-derivative probe. Nat. Biotechnol. 23, 577–583.

(18) Nesterov, E. E., Skoch, J., Hyman, B. T., Klunk, W. E., Bacskai, B. J., and Swager, T. M. (2005) In vivo optical imaging of amyloid aggregates in brain: Design of fluorescent markers. Angew. Chem., Int. Ed. 44, 5452–5456.

(19) Raymond, S. B., Skoch, J., Hills, I. D., Nesterov, E. E., Swager, T. M., and Bacskai, B. J. (2008) Smart optical probes for near-infrared fluorescence imaging of Alzheimer's disease pathology. Eur. J. Nucl. Med. Mol. Imaging 35 (SUPPL. 1), S93–S98.

(20) Li, Q., Lee, J. S., Ha, C., Chan, B. P., Yang, G., Wen, B. G., and Chang, Y. T. (2004) Solid-phase synthesis of styryl dyes and their application as amyloid sensors. Angew. Chem., Int. Ed. 43, 6331–6335.

(21) Ran, C., Xu, X., Raymond, S. B., Ferrara, B. J., Neal, K., Bacskai, B. J., Medarova, Z., and Moore, A. (2009) Design, synthesis, and testing of difluoroboron-derivatized curcumins as near-infrared probes for in vivo detection of amyloid-β deposits. J. Am. Chem. Soc. 131, 15257–15261.

(22) Ono, M., Ishikawa, M., Kimura, H., Hayashi, S., Matsumura, K., Watanabe, H., Shimizu, Y., Cheng, Y., Cui, M., Kawashima, H., and Saji, H. (2010) Development of dual functional SPECT/fluorescent probes for imaging cerebral β-amyloid plaques. Bioorg. Med. Chem. 20, 3885–3888.

(23) Zipfel, W. R., Williams, R. M., Christie, R., Nikitin, A. Y., Hyman, B. T., and Webb, W. W. (2003) Live tissue intrinsic emission microscopy using multiphoton-excited native fluorescence and second harmonic generation. Proc. Natl. Acad. Sci. U.S.A. 100, 7075–7080.

(24) Sutharsan, J., Dakanali, M., Capule, C. C., Haidekker, M. A., Yang, J., and Theodorakis, E. A. (2010) Rational design of amyloid binding agents based on the molecular rotor motif. ChemMedChem 5, 56–60.

(25) Haidekker, M. A., and Theodorakis, E. A. (2007) Molecular rotors - Fluorescent biosensors for viscosity and flow. Org. Biomol. Chem. 5, 1669–1678.

(26) Granzhan, A., and Teulade-Fichou, M.-P. (2009) Synthesis of mono- and bibrachial naphthalene-based macrocycles with pyrene or ferrocene units for anion detection. Tetrahedron 65, 1349–1360.

(27) Guram, A. S., Rennels, R. A., and Buchwald, S. L. (1995) A simple catalytic method for the conversion of aryl bromides to arylamines. Angew. Chem., Int. Ed. 34, 1348–1350.

(28) Wolfe, J. P., and Buchwald, S. L. (2000) Scope and limitations of the Pd/BINAP-catalyzed amination of aryl bromides. J. Org. Chem. 65, 1144–1157.

(29) Hartwig, J. F. (2008) Evolution of a fourth generation catalyst for the amination and thioetherification of aryl halides. Acc. Chem. Res. 41, 1534–1544.

(30) Sutharsan, J., Lichlyter, D., Wright, N. E., Dakanali, M., Haidekker, M. A., and Theodorakis, E. A. (2010) Molecular rotors: synthesis and evaluation as viscosity sensors. Tetrahedron 66, 2582–2588.

(31) LeVine, H., III (1993) Thioflavine T interaction with synthetic Alzheimer's disease β-amyloid peptides: Detection of amyloid aggregation in solution. Protein Sci. 2, 404–410.

(32) Iwatsubo, T., Odaka, A., Suzukishort, N., Mizusawa, H., Nukina, N., and Ihara, Y. (1994) Visualization of Aβ42(43) and Aβ40 in senile plaques with end-specific Aβ monoclonals: Evidence that an initially deposited species is Aβ42(43). Neuron 13, 45–53.

(33) Mann, D. M., Iwatsubo, T., Ihara, Y., Cairns, N. J., Lantos, P. L., Bogdanovic, N., Lannfelt, L., Winblad, B., Maat-Schieman, M. L., and

254

dx.doi.org/10.1021/cn200018v |ACS Chem. Neurosci. 2011, 2, 249–255

Rossor, M. N. (1996) Predominant deposition of amyloid-beta 42(43) in plaques in cases of Alzheimer's disease and hereditary cerebral hemorrhage associated with mutations in the amyloid precursor protein gene. *Am. J. Pathol. 148*, 1257–1266.

(34) Glabe, C. (2000) Does Alzheimer disease tilt the scales of amyloid degradation versus accumulation?. *Nat. Med. 6*, 133–134.

(35) We previously showed that probes based on the molecular rotor motif do not exhibit a significant change in fluorescence properties in the presence of monomeric Aβ42 peptides, suggesting that these probes do not associate with Aβ monomers.

(36) Zhao, X., and Yang, J. (2010) Amyloid-β peptide is a substrate of the human 20S proteasome. *ACS Chem. Neurosci. 1*, 655–660.

(37) Inbar, P., Li, C. Q., Takayama, S. A., Bautista, M. R., and Yang, J. (2006) Oligo(ethylene glycol) derivatives of thioflavin T as inhibitors of protein-amyloid interactions. *ChemBioChem 7*, 1563–1566.

(38) Lipinski, C. A., Lombardo, F., Dominy, B. W., and Feeney, P. J. (1997) Experimental and computational approaches to estimate solubility and permeability in drug discovery and development settings. *Adv. Drug Delivery Rev. 23*, 3–25.

(39) Habib, L. K., Lee, M. T. C., and Yang, J. (2010) Inhibitors of catalase-amyloid interactions protect cells from β-amyloid-induced oxidative stress and toxicity. *J. Biol. Chem. 285*, 38933–38943.

255

dx.doi.org/10.1021/cn200018v |*ACS Chem. Neurosci.* 2011, 2, 249–255